

Assessing the Sustainable Potential of Chemically Activated Crustacean Shells for Pilot-Scale Removal of Persistent Organic Pollutants in Contaminated Water: A Path Towards Environmental Sustainability

Abstract: Activated Carbon Samples were produced from periwinkle shells, clamshells, whelk shells, and a 1:1 composite of clam/whelk shells at a carbonization temperature of 450°C under limited-oxygen conditions and then activated using KOH at an activation temperature of 650°C. This produced Periwinkle, clam, whelk, and clam/whelk composite base activated carbons noted PSBAC, CSBAC, WSBAC, and CWSBAC respectively. The properties of these adsorbents were characterized by scanning electron microscopy energy dispersive X-ray analysis (SEM-EDX), Fourier Transform Infrared Spectrometry (FTIR), and physicochemical analysis. The examination indicated that CSBAC had the highest surface area at 1288 m²/g. The effect of the activated carbon dosages and contact times on the adsorption of PAHs was studied in batch adsorption experiments and the results indicated that CSBAC had the highest removal efficiency at 1g of 98.94%. The adsorption of PAHs was modeled using Langmuir, Freundlich, Henry, Elovich, and Janovich isotherms. The Freundlich and Langmuir models well described the sorption equilibrium data for PSBAC, CSBAC, and CWSBAC with PSBAC having a Langmuir maximum monolayer adsorption capacity of 31.688 mg/g. Henry Isotherm best described the sorption equilibrium data for WSBAC. Kinetic studies indicated that the adsorption processes of PAHs agreed well with a pseudo-second-order kinetic model.

Keywords: Persistent organic pollutants (POPs), Polycyclic Aromatic Hydrocarbons (PAHs), Crustacean Shells, KOH Activation, Periwinkle Shells, Clam Shells, Whelk Shells, Composite Shells, Freundlich Isotherm, Langmuir Isotherm, Henry Isotherm, Elovich Isotherm, Janovich Isotherm.

1. Introduction

Persistent organic pollutants (POPs) pose a significant threat to the environment and human health due to their long-lasting nature and potential for bioaccumulation. Polycyclic Aromatic Hydrocarbons (PAHs), a subset of POPs, are pressing issues that demand sustainable and efficient solutions as these compounds are among the most carcinogenic, mutagenic, and toxic contaminants [1]. PAHs generally enter water sources through road runoff, industrial wastewater, petroleum spills, and fossil fuel combustion [2]. During the last two decades, special attention has been paid to 16 polycyclic aromatic hydrocarbons (PAHs) listed by the United States Environmental Protection Agency (U.S. EPA) as priority pollutants due to their widespread environmental presence and their potential mutagenicity, teratogenicity, and carcinogenicity [3]. PAHs bioaccumulate in human and animal tissue and have been noted to have carcinogenic and mutagenic effects on humans ranging from non-cancer effects (skin disorders, effects on lung and blood in both humans and animals) to cancer effects (respiratory tract tumors, leukemia, lung cancer, and bladder cancer) [4]. They can adversely affect various reproductive, developmental, cardiovascular, nervous, and immune organs [5]. Exposure to PAHs during pregnancy has been linked to decreased birth weight and impaired child development [6]. In recent years, many methods such as chemical oxidation, photocatalytic advanced oxidation, and biological degradation have been used to remove PAHs from wastewater [7]. These treatment processes are chosen mainly based on the initial quality of the water, parameters established by regulations and proposed use [8]. Most methods have limitations, including the high operation and maintenance cost and incomplete removal of the organic pollutants. Adsorption is a widely used method for environmental protection, separation processes, gas purification, and wastewater treatment because it plays an important role in sustainable development [9]. Several adsorbent media such as activated carbon, biochar, and modified clay minerals have been largely used to remove PAHs from aqueous solution [10]. The choice of suitable adsorbent varies depending on its application. Cost, kinetics, compatibility, selectivity, capacity, and regenerability are important characteristics that affect the choice of adsorbents [8].

Materials used as adsorbents should be environmentally friendly, inexpensive, and simple to fabricate, exhibit high sorption capacity to remove the highest amount of pollutants, demonstrate high selectivity for specific contaminants, and be reusable and recyclable [11]. Activated carbon as a precursor for adsorption dates back to Ancient Egypt, where it was used to treat intestinal ailments, absorb unpleasant odours and tastes in water and write on papyrus. Hippocrates was documented as using wood charcoal to filter water to prevent bad taste and odour besides as a treatment for diseases such as anthrax, epilepsy, and Chlorosis [12]. Due to the high cost of available Commercial Activated Carbon, various studies focus on developing new low-cost Activated Carbon with properties comparable to that of commercial ones [13]. This has given rise to extensive studies on low-cost adsorbents ranging from plant seeds, stems, and husks to animal biomass. Activated carbon derived from biomass has gained wide acceptance in recent times as

they have been widely used in the removal of hazardous substances from the environment due to their nonhazardous nature and ability for regeneration [14]. [15] noted that 6 to 8 million tonnes of valuable crustacean shell waste are produced globally every year which makes it an environmentally abundant resource as precursors for activated carbon. Crustacean shells have vast amounts of chitin, a carbohydrate-based polymer that shows exceptional features such as biodegradability and biocompatibility and has been utilized as renewable, energy-efficient, cost-effective, and sustainable alternative materials. This study explores the feasibility and efficiency of chemically activated crustacean shells for pilot-scale remediation of polyaromatic hydrocarbon (PAHs) in contaminated water, with a focus on assessing their sustainable potential as it highlights the potential of these shells as a green and sustainable solution for tackling emerging environmental challenges.

2. Materials and Methods

2.1 Preparation of the adsorbent

Periwinkle shells (*Tympanotamus fuscatus*), West African Clam shells (*Galateaparadoxa*), and Whelk shells (*Buccium undatum*) were purchased from Town Market in Borokiri, Port Harcourt, Rivers State in Nigeria. They were soaked for four days in cleansing agents and warm water to remove dust, remaining organic particles, and soluble impurities. The shells were thoroughly washed in tap water and continuously agitated to remove the remaining impurities. The shells were dried in the sun for three days, carbonized at 450°C for 3 hours, and then powdered. The composite was prepared before chemical activation.

The samples were then soaked in 0.5 M KOH and mixed until a paste was formed then heated in a muffle furnace for 650°C for 2 hours. The resultant samples were cooled, and washed with deionized water to a pH of 6. The samples were then dried in the oven at 105°C for 6 hours and stored in air-tight containers.

2.2 Characterization

Attenuated Total Reflectance Fourier Transform Infrared Spectroscopy (ATR-FTIR) was performed using AGILENT TECHNOLOGIES CARY 630 FTIR CARY 630 ZnSe.

PART NO: -G804364002, MODEL NO: -MY19322004. The samples spectra were collected by placing the samples onto the ATR crystal and applying pressure to ensure good contact with the crystal. The spectra were then collected by shining an infrared beam onto the crystal and measuring the reflected light as a function of wavelength. The collected spectra were typically processed using software to remove any remaining baseline drift or noise. Scanning electron microscopy-energy dispersive X-ray analysis was performed using a PHENOM PRO X Serial no: MVE0224651193 Model no: 800-07334. The samples were mounted on stubs with adhesive carbon and coated in 20 nm Carbon with a QUORUM Q150R ES mini sputter coater, and then analyzed with a Phenom PRO-X SEM equipped with an Oxford XMax 50 Silicon Drift Energy Dispersive X-ray detector at 15KV under high vacuum. The specific surface area of the adsorbent was estimated according to the Sear method [16].

2.3 Preparation of PAHs contaminated water

Analytical-grade PAHs and high-performance liquid Chromatography-grade-
acetone(HPLC)fromLoba(LO)chemicewithdistilledwaterwereused for the adsorption
experiments. This was done in batches using 100ml volume flasks

UNDER PEER REVIEW

2.4 Batch Adsorption studies

2.4.1 Effect of Adsorbent Dosage

Specified adsorbent doses of 0.2, 0.4, 0.6, 0.8, and 1.0g at pH of 9 were added to 50ml water samples of 50mg/l initial PAH's concentration and attached to a mechanical shaker and the mixtures were agitated at 150rpm for different optimal period (90mins for PSBAC, 60mins for CSBAC and CWSBAC and 120 mins for WSBAC). Equilibrium studies were performed at room temperature (25°C). At the end of the agitation time, the mixtures were filtered through no. 542 Whatman filter paper. The filtrates were then separately analyzed for residual concentrations of PAHs using the GC/MS gas chromatograph. The equilibrium adsorption capacity (q_e) was obtained by using Equation (1).

$$q_e = \frac{(C_o - C_e)V}{M} \quad (1)$$

Where: q_e = quantity adsorbed (mg/g)

C_o and C_e = initial and equilibrium concentrations (mg/l) V =

Volume (L)

M = mass of adsorbent (g)

2.4.2 Effect of Contact time

The experiment was conducted to model the relationship between contact time and the adsorption capacity of activated samples. In a conical flask, 1 g of activated carbon sample was added to 50 ml PAHs standard solution at a concentration of 50 mg/L and was collected at 10-minute intervals from 10 minutes to 120 minutes at room temperature. PAH residues in the solution were extracted and analyzed.

2.4.3 PAHs Extraction method

The Liquid-Liquid extraction Technique used by [17] was used for extracting selected PAHs from sampled solutions. Dichloromethane (DCM) by Loba (LO) chemice analytical grade with 99.0% Purity was used for the extraction. Twenty-five (25) ml of dichloromethane was added, shaken vigorously for about 2 minutes to separate the organic layer, and vented occasionally to release pressure. The extracted mixture is decanted and repeated twice to ensure maximum PAH extraction. The solution waited six hours at room temperature for evaporation of DCM. 1g of sodium sulphate was introduced to adsorb any trace water before 1 ml of solution was decanted into the vial and ready for injection into Agilent 7890N GC/MS gas chromatography.

2.5 Sample Analysis Using GC-MS

1 ml of the analyte was introduced into the heated injector tube, vaporized, and mixed with a carrier gas. As the sample vapor is carried through the separation capillary column of 30 metres and film thickness and internal diameter of 250um by the carrier gas (helium), the analyte partitions between the gas and liquid phases according to the analyte components' solubility in the liquid at the column operating temperature which starts at 80°C for 2 minutes and increases at a rate of 30°C per minute until it peaks at 310°C. The rate of travel through the column is determined by the sample solubility in the stationary phase, the carrier gas flow rate, and the temperature. Each component travels at a characteristic rate. The sample

completely separated before arriving at the detector.

UNDER PEER REVIEW

2.6 Equilibrium modeling

The adsorption performance of the activated carbons was evaluated using the Henry, Langmuir, Freundlich, Elovich, and Jovanovic isotherm models. XLSTAT 2014 program was used for estimating coefficients based on a nonlinear optimization technique. Direct optimization method for nonlinear equations using iteration was used to minimize error in estimating model parameters. One of the isotherm models (Henry Isotherm) was a one-parameter model while the other four (Langmuir, Freundlich, Elovich, and Jovanovic isotherms) were two-parameter isotherm models.

2.7 Adsorption kinetics The adsorption kinetics were processed at varying time intervals using an initial concentration (50 mg/l) of PAHs. The procedures of kinetic experiments were identical to those of the equilibrium test. 1 g of crustacean-activated carbons (PSBAC, CSBAC, WSBAC, and CWSBAC) were mixed with 50 ml of PAH's simulated solution in top plastic containers which were then attached to a mechanical shaker at 150 rpm. The samples were taken at preset time intervals (5, 10, 20, 30, 40, 50, 60, 70, 80, 100 and 120 mins) and filtered. The concentrations of PAHs at these time intervals were measured. The adsorption capacity of the adsorbents at preset time, q_t , was calculated from Equation 2:

At time t , q_t (mg/g) was calculated using Equation 2

$$q_t = (q_o - q_t) \left(\frac{t}{t_m} \right)^V \quad (2)$$

q_t : uptake capacity of the material at time t (mg/g)

C_0 and C_t are the initial and final concentrations of the contaminated solution (mg/l) m : mass of adsorbent material (g)

V : volume of treated solution (l)

3. Results and Discussion

3.1 Results of the Adsorbent Characterization Experiments

3.1.1 The FTIR, SEM-EDX, and Surface Area of the Activated Carbon Prepared

The result in Table 1 indicated that the KOH-activated carbons displayed a large surface area for effective adsorption. [18] stated that the typical surface area of activated carbon samples ranges from 500 to 1500 m²/g. CSBAC had the highest surface area of 1288 m²/g

Table 1: Specific Area of activated crustacean shells

Parameter/Sample	PSBAC	CSBAC	WSBAC	CWSBAC
Specific Surface Area (m ² /g)	1275	1288	986	1270

The result of the FTIR in Table 2 and Figure 1 show that the spectra align with functional groups that were assigned to O-H, C-H, esters C=O, and amides C=O groups respectively indicating surface chemistry due to the activating agent with KOH. It also indicates low peak intensities of

the O-H, C-H, and C-O vibrations which is also consistent with KOH activation. This conforms to similar work by [19]

Table 2: FT-IR spectra data of the activated crustacean shells

Sample/band(cm^{-1})	O-H	C-H	C=O	C-O	C-O-C	M-O	Ar-H
CSBAC	3553	3345	1797	1122	1398	873	713
PSBAC	3518	3358	1789	1135	1389	864	704
WSBAC	3576	3389	1793	1135	1393	869	713
CWSBAC	3523	3336	1789	1126	1397	869	713

The SEM-EDX in Figure 2 indicated a broadly open pore structure demonstrating well-developed micropores. This is consistent with the activation of potassium hydroxide (KOH) which produces well-defined micropores to show the high adsorption capacity of the activated sample [20]. The elemental analysis in Table 3 confirmed a balanced ratio of oxygen and calcium, with CSBAC showing an oxygen concentration of 61.77 cm^{-1} and calcium at 38.23 cm^{-1} . The EDX analysis demonstrated that active carbons' calcium oxides (CaO) exist. CaO is a strong dehydrator, which absorbs water from the environment and increases the porosity of the treated activated materials, as observed in SEM studies.

Table 3: Elemental analysis of the activated crustacean shells by EDX

Sample/band(cm^{-1})	Element	Atomic concentration	Weight concentration
CSBAC	O	61.77	39.21
	Ca	38.23	60.79
PSBAC	O	70.97	49.39
	Ca	29.03	50.61
WSBAC	O	71.45	49.97
	Ca	28.55	50.03
CWSBAC	O	74.34	53.63
	Ca	25.66	46.37

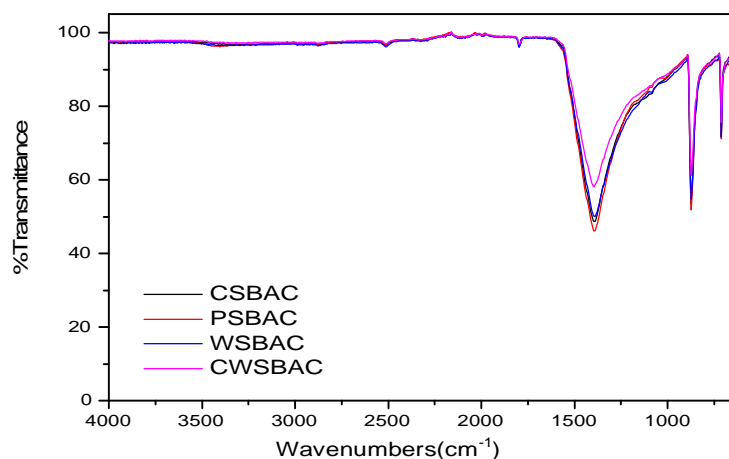


Figure 1: Stacked FT-IR spectra of KOH-treated activated carbons

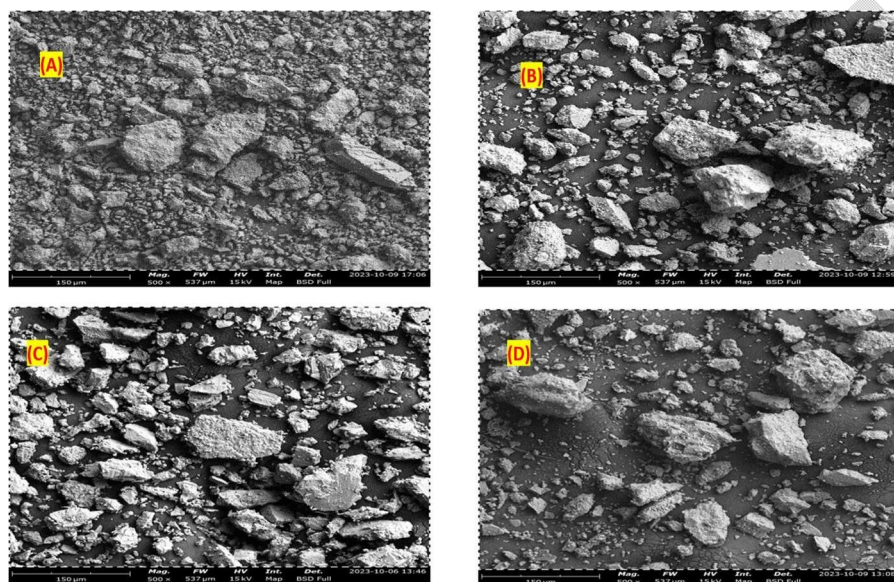


Figure 2: SEM Micrographs (at 150 μm) of CSBAC (A), PSBAC (B), WSBAC (C), and CWSBAC (D)

3.2 Results of Batch Adsorption studies

3.2.1 Effect of Adsorbent Dosage on Adsorption Efficiency

The graphical and tabular representation of the results obtained of the relationship between the mass of the adsorbent and the percentage removal of the adsorbate (Figure 3 and Table 4) revealed the increase in the mass of the adsorbent increased the percentage removal of the adsorbate. CSBAC indicated a percentage removal of approximately 84.14% at 0.2 g to 98.94% at 1 g. Similarly, CWSBAC increases from 83.14% to 98.91%, PSBAC from 82.03% to 98.54%, and WSBAC from 79.90% to 97.20%. This trend indicates that a higher mass of adsorbent provides more surface area and adsorption sites, enhancing the removal efficiency [21]. The steep slope observed at a lower mass of adsorbent (0.2 to 0.4 g) suggests that at lower adsorbent masses, the addition of adsorbent significantly improves the removal efficiency due to the increased availability of adsorption sites [22]. Beyond 0.4 g, the

slope tends to flatten, suggesting that the rate of increase in percentage removal becomes less effective as the system approaches equilibrium and the available adsorption sites become increasingly saturated [23].

3.3 Results of Equilibrium Concentration on Adsorption Capacity

The result in Figure 4 showed an increase in adsorption capacity in direct proportion to an increase in the equilibrium concentration for all adsorbents. It was observed that at an equilibrium concentration of approximately 2mg/l, the adsorption capacities of all activated samples were at 3mg/g with a slight disparity with WSBAC which was reported at 2mg/g. Further increase in equilibrium concentration revealed a wider disparity in the adsorption capacities of the activated samples. At an equilibrium concentration of approximately 7mg/l, CSBAC had the highest adsorption capacity of 9.2mg/g with CWSBAC and PSBAC showing a slightly lower adsorption capacity of approximately 9mg/g and 8.6mg/g respectively. There was a wide disparity in the adsorption capacity of WSBAC which was noted to be approximately 4.5mg/g. This suggests that WSBAC is less favorable for the adsorption of PAHs. Analysis of Variance (ANOVA) in Table 5 indicated that there was no significant difference in the adsorption capacities of all the activated carbons subjected to investigation despite the lower adsorption capacity of WSBAC (F-value(3,16)=0.008, p-value= 0.999)

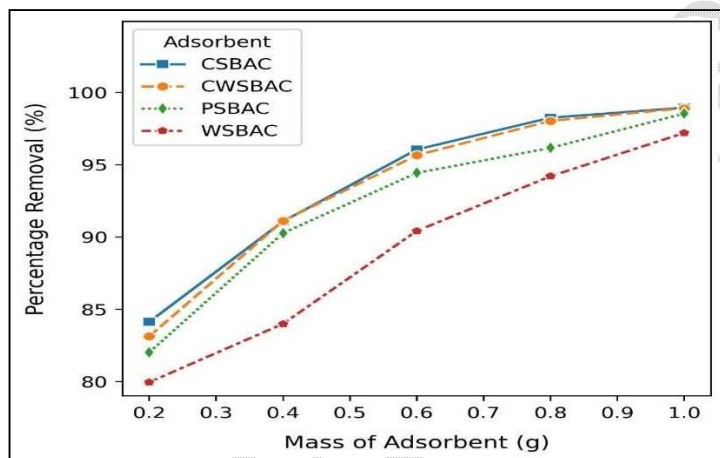


Figure 3: Effect of adsorbent mass on percentage removal.

Table 4: Efficiency of adsorption (Percentage Removal) at adsorbent dosage of 1g

Sample	Efficiency (%)	Ranking
CSBAC	98.94	1
CWSBAC	98.91	2
PSBAC	98.54	3
WSBAC	97.20	4

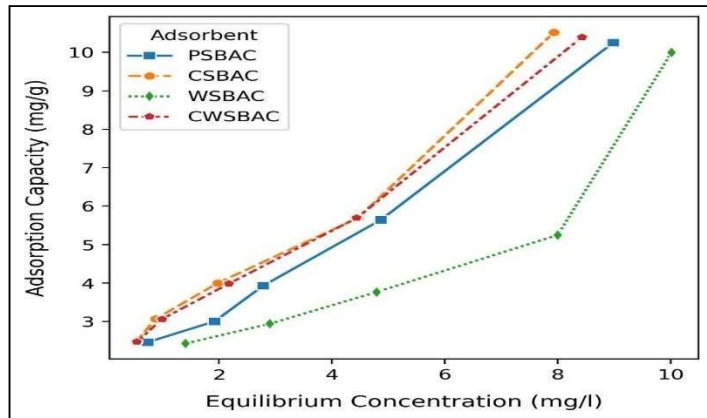


Figure 4: Adsorption Capacity against the equilibrium concentration

Table 5: ANOVA for Adsorption Capacity.

Source	DF	Sum of squares	Mean squares	F	Pr > F
Model	3	0.226	0.075	0.008	0.999
Error	16	159.421	9.964		
Corrected Total	19	159.648			

Computed against model $Y = \text{Mean}(Y)$

3.3.1 Effect of Contact time on adsorption capacity

The result from Figure 5 showed that all four adsorbents exhibited increasing adsorption capacities as the contact time increased. As contact time increases, a general upward trend in adsorption capacity is observed for all adsorbents, although the rate of increase varies among them [24]. WSBAC showed a steady, continuous increase in adsorption capacity reaching approximately 2.362 mg/g after 100 minutes without attaining equilibrium adsorption capacity. In contrast, CSBAC, CWSBAC, and PSBAC exhibit quicker adsorption rates initially, plateauing around 60 to 90 minutes. The result indicates that the adsorption sites for CSBAC, CWSBAC, and PSBAC may become saturated, as extending the contact time beyond this period does not significantly increase their adsorption capacities. This result indicates that a progression in contact time resulted in a decrease in active sites, and the formation of strong bonds between the adsorbate and adsorbent, leading to a slowdown in the process before equilibrium [25]. CSBAC achieves the highest adsorption capacity of approximately 2.49 mg/g, followed by CWSBAC with a capacity of around 2.473 mg/g, and PSBAC with about 2.263 mg/g. The analysis of Variance (ANOVA) in Table 6 shows significant differences in the adsorption capacities for the four base-activated carbons (F-value(3,31)=9.408, p-value < 0.0001). This provided sufficient evidence to state that the adsorption capacities for the four base-activated carbons were different over the contact time. The Tukey test results in Table 7 revealed that CSBAC, CWSBAC, and PSBAC belong to group A, indicating no significant differences in their adsorption capacities among these three adsorbents. However, WSBAC belongs to group B, indicating its adsorption capacity is significantly lower compared to the other three adsorbents.

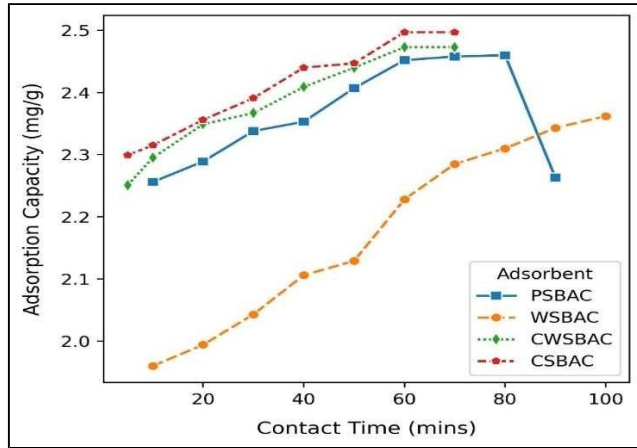


Figure 5: Adsorption Capacity against the contact time

Table 6: Analysis of Variance of the Adsorption Capacity based on Contact Time for the different Base activated carbon.

Source	DF	Sum of squares	Mean squares	F	Pr > F
Model	3	0.313	0.104	9.408	0.000
Error	31	0.344	0.011		
Corrected Total	34	0.657			

Computed against model $Y = \text{Mean}(Y)$

Table 7: Tukey Test

Category	LS means	Standard error	Lower bound (95%)	Upper bound (95%)	Groups
CSBAC	2.405	0.037	2.329	2.481	A
CWSBAC	2.382	0.037	2.306	2.458	A
PSBAC	2.364	0.035	2.292	2.436	A
WSBAC	2.176	0.033	2.108	2.244	B

3.4 Regression Modeling

The regression modeling results indicate a highly effective model for predicting percentage removal based on the mass of the adsorbent used. The goodness of fit, ANOVA, and model parameters for base-activated carbon reveal significant findings. The goodness of fit for the regression model in Table 8 shows an R^2 value of 0.921 and an adjusted R^2 of 0.900, indicating that the model explains 92.1% of the variability in percentage removal. The adjusted R^2 , which accounts for the number of predictors, confirms the model's robustness. The Mean Squared Error (MSE) is 3.976, and the Root Mean Squared Error (RMSE) is 1.994, both demonstrating high accuracy in the model's predictions. The Durbin-Watson statistic (DW) of 1.432 suggests no significant autocorrelation in the residuals, supporting the model's reliability.

The ANOVA results in Table 9 further validate the model's significance, with a model F-value of 43.662 and a p-value of less than 0.0001. This high F-value indicates that the regression model is

highly significant, and at least one of the predictors (mass of adsorbent or type of adsorbent) significantly explains the variation in percentage removal. The model parameters for activated carbon in Table 10 provided detailed insights into the effects of each predictor. The intercept is 77.251 with a standard error of 1.300 and a t-value of 59.427 ($p < 0.0001$), indicating a substantial baseline percentage removal. The carbon dosage parameter has a value of 19.847, with a standard error of 1.576 and a t-value of 12.590 ($p < 0.0001$), indicating a strong positive correlation between the mass of adsorbent and percentage removal. The type of adsorbent also significantly affects the percentage removal. CSBAC increases percentage removal by 4.533 units, CWSBAC by 4.212 units, and PSBAC by 3.129 units compared to the reference adsorbent (WSBAC), which has a coefficient of 0.000. The standard errors for these parameters are 1.261, with t-values indicating significant effects (p-values of 0.003 for CSBAC, 0.004 for CWSBAC, and 0.025 for PSBAC).

Table 8: Goodness of fit

Observations	20.000
Sum of weights	20.000
DF	14.000
R ²	0.945
Adjusted R ²	0.925
MSE	0.631
RMSE	0.794
DW	2.218

Table 9: ANOVA

Source	DF	Sum of squares	Mean squares	F	Pr > F
Model	5	150.813	30.163	47.798	<0.0001
Error	14	8.835	0.631		
Corrected Total	19	159.648			

Computed against model $Y = \text{Mean}(Y)$

Table 10: Model Parameters (Base activated Carbon)

Source	Value	Standard error	t	Pr > t	Lower bound (95%)	Upper bound (95%)
Intercept	-2.138	2.397	-0.892	0.387	-7.279	3.002
Carbon Dosage	1.782	2.136	0.834	0.418	-2.799	6.363
Ce	1.097	0.206	5.333	0.000	0.656	1.538
Adsorbent-CSBAC	2.760	0.685	4.027	0.001	1.290	4.231
Adsorbent-CWSBAC	2.555	0.663	3.851	0.002	1.132	3.978
Adsorbent-PSBAC	1.898	0.597	3.182	0.007	0.619	3.178
Adsorbent-WSBAC	0.000	0.000				

3.5 Adsorption Isotherm Models

From the results from Table 11, The maximum adsorption capacity for monolayer Q_m was compared between Langmuir and Janovich isotherms, and it was noted that Langmuir Isotherm presented the highest adsorption capacities for PSBAC, CSBAC and CWSBAC with values of 31.688, 18.335 and 18.743 mg/g respectively while Janovich Isotherm presented a higher maximum capacity for WSBAC at 10.362 mg/g.

It can be noted that the resultant Freundlich exponent values n for PSBAC, CSBAC, and CWSBAC were 1.329, 1.633, and 1.621 respectively. This signifies high adsorption rate as the ideal values for the exponent n lying between 0 and 10 suggest favorable adsorption [26] [27]. This implies that the activated samples are heterogeneous with sites of varying affinities, and have a varied surface with multiple adsorption sites, each with different adsorption energies which is better captured by the Freundlich model than by other models [28]. The Henry isotherm model best described the adsorption behavior of WSBAC with R^2 values of 0.835 and a Henry constant (K_{HE}) of 0.871. This suggests that the adsorption process for WSBAC follows a linear isotherm, indicative of low-concentration adsorption states or infinite dilution, where the adsorbate molecules do not interact with each other, and the surface sites are uniformly available [29].

Table 11: Isotherm Models

Number of parameters	Isotherm Model Type	Model Parameters	Activated samples			
			PSBAC	CSBAC	WSBAC	CWSBAC
One-Parameter	Henry	K_{HE}	1.187	1.376	0.871	1.301
		R^2	0.939	0.886	0.835	0.892
Two-Parameters	Langmuir	Q_m	31.688	18.335	9.133	18.743
		b	0.051	0.144	2.131	0.131
	Freundlich	R^2	0.951	0.898	0.834	0.917
		K_f	1.901	2.770	0.908	2.649
		n	1.329	1.633	1.020	1.621
		R^2	0.966	0.940	0.831	0.956
	Elovich	β	0.339	0.380	0.317	0.380
		α	5.867	9.306	3.406	8.664
		R^2	0.742	0.787	0.512	0.799
	Jovanovic	Q_m	19.316	13.416	10.362	13.322
K_f		0.082	0.170	0.000	0.163	
R^2		0.951	0.897	0.834	0.915	

Q_m = Maximum monolayer adsorption capacity (mg/g), K_{HE} = Henry's adsorption constant, b = Langmuir constant (L/mg), R^2 = Correlation Coefficient, K_f = Affinity factor (mg/g)*(L/mg)^{1/n}, n = Freundlich exponent, α = initial rate constant (mg/g * min), β = desorption constant (mg/g)

3.5.1 Adsorption Kinetics Table 12 indicated that across all activated carbons, the second-order kinetic model generally provided a better fit for the adsorption data, as evidenced by higher R^2 values

compared to the first-order model. This conforms with previous findings reported by [30] and [31]. The rate constants in the second-order model, despite varying, generally suggested more accurate and faster adsorption processes, reinforcing the suitability of the second-order model in describing the kinetics of adsorption for these activated carbons. The review of sorption kinetics done by [32] concluded the pseudo-second-order equation might be applied to chemisorption processes with a high degree of correlation. This indicates that chemisorption is the mechanism identified in this research.

Table 12: Kinetic Models

Carbon Activator	Model Parameters	First-Order	Second Order
CSBAC	q _e	2.4231	2.4662
	K	0.5770	0.8937
	R ²	0.9994	0.9997
CWSBAC	q _e	2.4044	2.4513
	K	0.5333	0.7822
	R ²	0.9995	0.9998
PSBAC	q _e	2.3797	2.4248
	K	0.2881	0.4946
	R ²	0.9992	0.9993
WSBAC	q _e	2.2119	2.3306
	K	0.1959	0.1677
	R ²	0.9972	0.9987

4. Conclusion

This study provides valuable insights into the potential use of Chemically activated crustacean shells as a viable option for addressing PAH contamination in water. The experimental analyses established that the activated carbons prepared from periwinkle shells, clam shells, whelk shells, and composite clam/whelk shells have good morphology and physicochemical properties for adsorption. The removal of PAHs was influenced by the operational parameters which were contact time and adsorbent dosage. Freundlich isotherm adequately described the sorption for CSBAC, CWSBAC, and PSBAC, while the sorption using WSBAC was adequately interpreted by Henry isotherm. Further analyses into the adsorption kinetics revealed the processes followed pseudo-second-order kinetics. It has shown that modified Crustacean shells are excellent and eco-friendly alternatives for the removal of PAHs from the aquatic environment with emphasis on the importance of sustainability in pollution management practices.

References

1. Zhang W, Chaohai W, Xinsheng C, Jingying H, Ying C, Man R, Bo Y, Pingan P and Jiamo F (2012) The behaviors and fate of polycyclic aromatic hydrocarbons (PAHs) in a coking wastewater treatment plant <http://dx.doi.org/10.1016/j.chemosphere.2012.02.076>
2. Ugochukwu C. U and Ochonogor A (2018) Groundwater contamination by polycyclic aromatic hydrocarbon due to diesel spill from a telecommunication station in a Nigerian City: assessment of human health risk exposure. <https://doi.org/10.1007/s10661-018-6626-2>
3. Saber A. N, Haifeng Z, Ashrafulland Min Y (2021). Occurrence, fates, and carcinogenic risks of substituted polycyclic aromatic hydrocarbons in two coking wastewater treatment systems. <https://doi.org/10.1016/j.scitotenv.2021.147808>
4. Rajasekhar B, Indumathi M. N and Suresh K. G (2018) Human health risk assessment of groundwater contaminated with petroleum PAHs using Monte Carlo simulations: A case study of an Indian metropolitan city. <https://doi.org/10.1016/j.jenvman.2017.09.078>
5. Choi, J. W., Kim, M., Song, G., Kho, Y., Choi, K., Shin, M. and Kim, S. (2023). Toxicokinetic analyses of naphthalene, fluorene, phenanthrene, and pyrene in humans after single oral administration. *Science of The Total Environment*, 870, 161899. <https://doi.org/10.1016/j.scitotenv.2023.161899>
6. Ite A. E, Thomas A. H, Clement O. O, Ekpeme R. A and Iniemem J. Inim (2018) Petroleum Hydrocarbons Contamination of Surface Water and Groundwater in the Niger Delta Region of Nigeria. *Journal of Environment Pollution and Human Health*, vol. 6, no. 2 pp 51-61. <http://dx.doi.org/10.12691/jephh-6-2-2>
7. Qiao, K., Tian, W., Bai, J., Dong, J., Zhao, J., Gong, X., & Liu, S. (2018). Preparation of biochar from *Enteromorpha prolifera* and its use for removing polycyclic aromatic hydrocarbons (PAHs) from aqueous solution. *Ecotoxicology and Environmental Safety*, 149, 80-87. <https://doi.org/10.1016/j.ecoenv.2017.11.027>
8. Akomah U, Nwaogazie I. L and Akaranta O (2021) A Review on Current Trends in Heavy Metal Removal from Water between 2000-2021. *International Journal of Environment and Climate Change* 11(12): 67-90. <https://doi.org/10.9734/ijecc/2021/v11i1230557>
9. Azizian S and Eris S. (2020). Adsorption isotherms and kinetics. *Interface Science and Technology*, 33, 445-509. <https://doi.org/10.1016/B978-0-12-818805-7.00011-4>
10. Lamichhane, S., Bal Krishna, K., and Sarukkalige, R. (2016). Polycyclic aromatic hydrocarbons (PAHs) removal by sorption: A review. *Chemosphere*, 148, 336-353. <https://doi.org/10.1016/j.chemosphere.2016.01.036>
11. Sahoo T. R and Prelo B (2020) Nanomaterials for the Detection and Removal of Wastewater Pollutants. <https://doi.org/10.1016/B978-0-12-818489-9.00007-4>
12. Gayathiri M, Thiruchelvi P, Lee K. T. and Kumar S (2022) Activated carbon from biomass waste precursors: Factors affecting production and adsorption mechanism. <https://doi.org/10.1016/j.chemosphere.2022.133764>

13. El Gamal, M., Mousa, H. A., El-Naas, M. H., Zacharia, R., & Judd, S. (2018). Bioregeneration of activated carbon: A comprehensive review. *Separation and Purification Technology*, 197, 345-359. <https://doi.org/10.1016/j.seppur.2018.01.015>
14. Ani, J.U., Akpomie, K.G., Okoro, U.C., Aneke L.E, Onukwuli O.D and Ujam O.T (2020). Potential of activated carbon produced from biomass materials for sequestration of dyes, heavy metals, and crude oil components from aqueous environment. *Appl Water Sci* 10, 69. <https://doi.org/10.1007/s13201-020-1149-8>
15. Vicente, F.A., Ventura, S.P., Passos, H., Dias, A.C., Torres-Acosta, M.A., Novak, U., and Likozar, B. (2022). Crustacean waste biorefinery as a sustainable cost-effective business model. *Chemical Engineering Journal*, 442, 135937. <https://doi.org/10.1016/j.cej.2022.135937>
16. Abate G. Y, Adugna N. A, Adere T. Hand Desiew M. G (2020). Adsorptive removal of malachite green dye from aqueous solution onto activated carbon of Catha edulis stem as a low cost bio-adsorbent. <https://doi.org/10.1186/s40068-020-00191-4>
17. Assad A. A, Gaber S. E and Jahin H. S (2019) Removal of Polycyclic Aromatic Hydrocarbons from Water Utilizing Activated Carbons. *World Journal of Chemistry* 14 (1):22-32. DOI:10.5829/idosi.wjc.2019.22.32
18. Ngu, L. H. (2023). Carbon Capture Technologies. *Encyclopedia of Sustainable Technologies (Second Edition)*, 358-377. <https://doi.org/10.1016/B978-0-323-90386-8.00028-0>
19. Eke-emezie, N., Etuk, B.R., Akpan, O.P and Okechukwu C.C (2022). Cyanide removal from cassava wastewater onto H₃PO₄ activated periwinkle shell carbon. *Appl Water Sci* 12, 157. <https://doi.org/10.1007/s13201-022-01679-3>
20. Iwanow M, Tobias G, Volker S and Burkhard K (2020) Activated carbon as catalyst support: precursors, preparation, modification and characterization. *Beilstein J. Org. Chem.* 2020, 16, 1188–1202. <https://doi.org/10.3762/bjoc.16.104>
21. Huang, Y., Fulton, A.N., and Keller, A.A. (2016). Simultaneous removal of PAHs and metal contaminants from water using magnetic nanoparticle adsorbents. *Science of The Total Environment*, 571, 1029-1036. <https://doi.org/10.1016/j.scitotenv.2016.07.093>
22. Wang Z., Zheng X., Wang, Y., Lin, H., and Zhang, H. (2022). Evaluation of phenanthrene removal from soil washing effluent by activated carbon adsorption using response surface methodology. *Chinese Journal of Chemical Engineering*, 42, 399-405. <https://doi.org/10.1016/j.cjche.2021.02.027>
23. Aravind K, Krithiga . J, Vijai A. T, Sathish. K, Karthick R. N, Renita, A., Hosseini-Bandegharai A., Praveenkumar T., Rajasimman M., Bhat, N., and Dutta, S. (2021). Kinetics and regression analysis of phenanthrene adsorption on the nanocomposite of CaO and activated carbon: Characterization, regeneration, and mechanistic approach. *Journal of Molecular Liquids*, 334, 116080. <https://doi.org/10.1016/j.molliq.2021.116080>
24. Agarwal, B., Majumder C.B., and Thakur P.K. (2013). Simultaneous co-adsorptive removal of phenol and cyanide from binary solution using granular activated carbon. *Chemical Engineering Journal* 228: 655–64. doi:10.1016/j.cej.2013.05.030.

25. Asokogene O.F, Muhammad A.A.Z, Zainul A.Z, Idris M.M, Surajudeen A and Usman A. El-Nafaty (2020): Equilibrium and kinetics of phenol adsorption by crab shell chitosan, *Particulate Science and Technology*, DOI:10.1080/02726351.2020.1745975. <https://doi.org/10.1080/02726351.2020.1745975>
26. Tran, H. N., You, S., Hosseini-Bandegharai, A. and Chao, H. (2017). Mistakes and inconsistencies regarding adsorption of contaminants from aqueous solutions: A critical review. *Water Research*, 120, 88-116. <https://doi.org/10.1016/j.watres.2017.04.014>
27. Rolph C.A, Jefferson B, Hassard F and Villa R (2018) Metal dehydro removal from drinking water by adsorption onto filtration media: mechanisms and optimization. <http://dx.doi.org/10.1039/C8EW00056E>
28. Kumar, J. A., Amarnath, D. J., Sathish, S., Jabasingh, S. A., Saravanan, A., Hemavathy, R., Anand, K. V., and Yaashikaa, P. (2019). Enhanced PAHs removal using pyrolysis-assisted potassium hydroxide induced palm shell activated carbon: Batch and column investigation. *Journal of Molecular Liquids*, 279, 77-87. <https://doi.org/10.1016/j.molliq.2019.01.121>
29. Ayawei N, Augustus N.E, and Donbebe W (2017). Modelling and Interpretation of Adsorption Isotherms. <https://doi.org/10.1155/2017/3039817>
30. Awoyemi, A. (2011). Understanding the adsorption of polycyclic aromatic hydrocarbons from aqueous phase onto activated carbon. Toronto (ON): University of Toronto.
31. Cabal, B., Budinova, T., Ania, C.O., Tsyntsarski, B., Parra, J.B., and Petrova, B. (2009). Adsorption of naphthalene from aqueous solution on activated carbons obtained from bean pods. *Journal of Hazardous Materials*, 161(2-3), 1150-1156. <https://doi.org/10.1016/j.jhazmat.2008.04.108>
32. Lamichhane, S., Bal Krishna, K., and Sarukkalige, R. (2016). Polycyclic aromatic hydrocarbons (PAHs) removal by sorption: A review. *Chemosphere*, 148, 336-353. <https://doi.org/10.1016/j.chemosphere.2016.01.036>